On the *Z*−*E* Photoisomerization of Chiral 2-Pentenoate Esters: Stationary Irradiations, Laser-Flash Photolysis Studies, and Theoretical Calculations

Elena García-Expósito, Rafael González-Moreno, Marta Martín-Vilà, Elena Muray, Joan Rifé, José L. Bourdelande,*,† Vicenç Branchadell,*,‡ and Rosa M. Ortuño*

Departament de Química, Universitat Autònoma de Barcelona, 08193 Bellaterra, Barcelona, Spain

rosa.ortuno@uab.es

Received April 12, 2000

Chiral pentenoates **1**−**3** in both *Z* and *E* isomeric forms underwent stationary irradiations in several solvents and in the presence of different photosensitizers. The photostationary-state ratio has been determined for each *Z*/*E* couple showing a predominance of the thermodynamically more stable isomer for **1** and **3**. Moreover, transient species were generated by pulsed laser excitation and detected by their characteristic ultraviolet absorptions, being the first time that enoate-originated triplets are detected. Stern−Volmer quenching studies afforded a quantitative measure for the efficiency of the photosensitization processes induced by benzophenone or acetophenone and allowed the determination of the corresponding quenching rate constants. Density functional calculations permitted the determination of the geometries and the energies of the diastereomeric excited states. Two diastereomeric orthogonal and two diastereomeric planar structures result as a consequence of the presence of a chiral substituent. The orthogonal triplets are the energy minima in all cases, whereas the planar triplets are the transition states linking these orthogonal structures, the corresponding energy barriers being 8−10 kcal mol^{-1} for enoates **1**−**3**. The computed S_0 to T_1 excitation energies show a trend which is consistent with the quenching rate constants. On the other hand, the triplet lifetimes determined for **1** and **2** are unusually long (1−20 μs) if compared with the data already described for several enones, in the range of nanoseconds. This fact has been rationalized from calculations of spin−orbit coupling at several points of the T_1 potential energy surface. This coupling is maximum for structures with a torsional angle close to 45°, which are 4−5 kcal mol^{-1} above the minima of T_1. Calculations done on the hypothetical aldehyde **4** and methyl vinyl ketone show much lower energy barriers, thus accounting for the shorter lifetimes reported for enone triplets.

Introduction

Photochemically promoted *Z*−*E* isomerization of olefins is a well-known process that plays an important role in biological phenomena such as vision.[1] In other instances, *Z*−*E* arrangement has been employed for synthetic purposes to dispose of significant amounts of the minor isomeric olefins produced under thermal conditions.[2]

Several studies have been carried out to determine the features of the photochemically promoted *Z*−*E* isomerization of simple olefins, i.e., the excited states involved and the mechanism. These rearrangements often proceed via triplet energy transfer in photosensitized processes.[3] Olefins conjugated to aromatic rings also have been investigated, especially in laser flash-photolysis (LFP) studies which allow the detection of the transient species and the measurement of their lifetime as well as the efficiency of the sensitizers used.[4]

The sensitized *Z*−*E* isomerization of alkenes is generally thought to involve generation of either the *Z* or *E* $^3(\pi,\pi^*)$ state, depending on the configuration of the ground-state molecule, followed by decay of each of these intermediates to a common orthogonal species by loss of vibrational energy and twisting about the carbon−carbon bond. Studies carried out on alkenes show that in most cases the transfer of triplet energy from the sensitizer to both the *Z* and *E* isomers is nonvertical, i.e., the alkene is excited from the ground state directly to a twisted geometry.[3c,5,6]

Theoretical calculations have been carried out to rationalize the experimental findings. It is accepted that the rate of T_1−S_0 intersystem crossing (isc) depends on the energy gap between both states and on the spin−

† E-mail: jl.bourdelande@cc.uab.es.
‡ E-mail: vicenc@klingon.uab.es.

(1) Honig, B.; Ebrey, T. G. *Annu. Rev. Biophys. Bioeng.* **1974**, *3*, 151.
(2) (a) A classical example: *E* to *Z* isomerization of *β*-ionol. Ramamurthy, V.; Liu, R. S. H. *J. Am. Chem. Soc.* **1976**, *98*, 2935. (a) A recent example: *Z* to *E* isomerization of *N*,*O*,*O*-triacetyl-*erythro*- and *threo*-C_{18}-sphingosines. Dondoni, A.; Perrone, D.; Turturici, E. *J. Chem. Soc., Perkin Trans. 1* **1997**, 2389.
(3) (a) Hammond, G. S.; Saltiel, J.; Lamola, A. A.; Turro, N. J.; Bradshaw, J. S.; Cowan, D. O.; Counsell, R. C.; Vogt, V.; Dalton, C. *J. Am. Chem. Soc.* **1964**, *86*, 3197. (b) Lee, E. K. C.; Denschlang, H. O. Haninger, G. A., Jr.. *J. Chem. Phys.* **1968**, *48*, 4547. (c) Saltiel, J.; Neuberger, K. R.; Wrighton, M. *J. Am. Chem. Soc.* **1969**, *91*, 3658.
(4) See, for instance: (a) Furuchi, H.; Arai, T.; Kuriyama, Y.; Sakuragi, H.; Tokumaru, K. *Chem. Phys. Lett.* **1989**, *162*, 211. (b) Karatsu, T.; Hiresaki, T.; Arai, T.; Sakuragi, H.; Tokumaru, K.; Wirz, J. *Bull. Chem. Soc. Jpn.* **1991**, *64*, 3355. (c) Saltiel, J.; Wang, S.; Ko, D.-H.; Gormin, D. A. *J. Phys. Chem. A* **1998**, *102*, 5383.
(5) Snyder, J. J.; Tise, F. P.; Davis, R. D.; Kropp, P. J. *J. Org. Chem.* **1981**, *46*, 3609.
(6) (a) Hammond, G. S.; Saltiel, J. *J. Am. Chem. Soc.* **1963**, *85*, 2516. (b) Herkstroeter, W. G.; Hammond, G. S. *J. Am. Chem. Soc.* **1966**, *88*, 4769. (c) Stephenson, L. M.; Hammond, G. S. *Angew. Chem., Int. Ed. Engl.* **1969**, *8*, 261.

10.1021/jo000549g CCC: $19.00
Published on Web 09/21/2000

orbit coupling (SOC). Since this gap is minimum at the perpendicular twisted geometry (of D_{2d} symmetry for ethylene itself), this geometry was generally considered[7] as that one at which isc occurs. Caldwell et al.[8] calculated SOC matrix elements for alkenes finding that SOC varies greatly with the angle of twist around the C=C bond, being zero at the 90° geometry and maximal at twist angles of 45 and 135°. Moreover, pyramidalization at one of the trigonal centers also improves SOC. Thus, in a series of alkenes, those triplets showing the shortest lifetimes must closely approach the structure in which a good compromise between the T_1-S_0 gap and SOC is reached. This is in good agreement with the experimental results observed for different cyclic conjugated enones (vide infra).[9] More recently, SOC in ethylene and its role in triplet to singlet radiationless transition has been analyzed by several authors.[10]

On the other hand, irradiation at shorter wavelengths and detection of short-lived transients has become feasible with modern LFP equipment, and therefore other kind of olefins, such as cyclic enones, have been recently investigated. Although small-sized rings cannot undergo *Z*−*E* isomerization, twisted triplets have been invoked to explain the formation of *trans*-fused bicyclic structures upon [2 + 2] photocycloaddition of alkenes to cyclohexenones.[11] In the initial studies done by Bonneau,[12] the triplet π,π^* excited states of several enones were generated by pulsed laser excitation, at either 265 or 353 nm, and showed absorption at 260−280 nm. Lifetimes were in the nanosecond domain. It was proposed that, for enones where twisting in the ground state is structurally feasible, the orthogonal triplet state should be readily accessible and would have a short lifetime because of strong coupling with the ground state at the perpendicular configuration. Structural constraints to twisting would be expected to increase the lifetime of the enone, triplet and indeed testosterone shows a lifetime of 400 ns. This fact was also observed by Kelly and McMurry[13a] for rigid enones and explained on the basis of both electronic and steric factors hindering twisting.[13a,b]

In 1991, Schuster and Bonneau described the results of an extensive study carried out in collaboration, in which data concerning energies and lifetimes of reactive triplets from several cyclic conjugated enones were reported.[9] The described results reinforced the original proposal of Bonneau that the enone transients with lifetimes of nanoseconds are twisted π,π^* triplet states. For testosterone and rigid bicyclic enones, the T_1-S_0 gap is large and SOC is poor, resulting in relatively long triplet lifetimes.

Beside all these studies on enones, there is a lack of information concerning the transients involved in the *Z*−*E* photoisomerization of α,β-unsaturated esters since, to the best of our knowledge, neither experimental nor calculated data have been reported. Therefore, we decided to investigate the behavior of pentenoates **1**−**3** under *Z*−*E* photoisomerization conditions. These compounds have the *S* configuration at C-4 and differ from each other in the substitution at olefinic *C-2*: H in ester **1**,[14] methyl in **2**,[15] and acetylamino in **3**,[16] the latter containing a capto-dative system. They are easily prepared from D-glyceraldehyde as a chiral precursor. These compounds have been used in conjugate additions,[17a,b] concerted additions,[17c] and cycloadditions,[17d,e,f,g,i] providing adducts in high diastereomeric excesses. These adducts have been employed as building blocks in the asymmetyric synthesis of a variety of products.[16,17b,c,h,18]

It is well-known that the diastereoselectivity in thermal reactions is determined by the energy difference between the diastereomeric transition states leading to each isomer, this difference being determined by the chirality of the reactants. Nevertheless, there is very little knowledge about the influence that the stereogenic centers in the substrates exert on the energies of the excited states and, by extension, on the stereochemical outcome of photoinduced reactions. For this reason, we undertook the present study.

Thus, in this paper, we report the results on the photochemical and photophysical behavior of enoates **1**−**3** in *Z*−*E* isomerizations. Stationary irradiations led to determination of the influence of the solvent and of the photosensitizers, as well as the $(Z/E)_{PSS}$ ratio for each compound. LFP allowed the identification of the generated triplet transients and the determination of their lifetimes, which were unexpectedly long, in the range of microseconds. The quenching rate constants for benzophenone and acetophenone were also determined. Theoretical calculations, done by Density Functional methods (DFT), led to a study of the T_1 potential energy surfaces and to the geometries and the energies of the diastereomeric orthogonal or planar triplets and their interconversion barriers. These data are in good agreement with the experimentally observed role of the different sensitiz-

(7) (a) Saltiel, J.; Charlton, J. L. In *Rearrangements in Ground and Excited States*; de Mayo, P., Ed.; Academic Press: New York, 1980; p 25. (b) Caldwell, R. A. *Pure Appl. Chem*. **1984**, *56*, 1196. (c) Caldwell, R. A.; Cao, C. V. *J. Am. Chem. Soc.* **1982**, *104*, 6174. (c) Bonneau, R.; Herran, B. *Laser Chem*. **1984**, *4*, 151. (d) Goerner, H.; Schulte-Frohlinde, D. *J. Phys. Chem*. **1981**, *85*, 1835.

(8) Caldwell, R. A.; Carlacci, L.; Doubleday, C. E., Jr.; Furlani, T. R.; King, H. F.; McIver, J. W., Jr. *J. Am. Chem. Soc.* **1988**, *110*, 6901.

(9) Schuster, D. I.; Dunn, D. A.; Heibel, G. E.; Brown, P. B.; Rao, J. M.; Woning, J.; Bonneau, R. *J. Am. Chem. Soc.* **1991**, *113*, 6245.

(10) (a) Geheim, B.; Peyerimhoff, S. D. *J. Phys. Chem. A* **1996**, *100*, 19257. (b) Danovich, D.; Marian, C. M.; Neuheuser, T., Peyerimhoff, S. D.; Shaik, S. *J. Phys. Chem. A* **1998**, *102*, 5923.

(11) (a) Bowman, R. M.; Calvo, C.; McCollough, J. J.; Rasmussen, P. W.; Snyder, F. F. *J. Org. Chem*. **1972**, *37*, 2084. (b) Schuster, D. I.; Greenberg, M. M.; Nuñez, I. M.; Tucker, P. C. *J. Org. Chem*. **1983**, *48*, 2615.

(12) Bonneau, R. *J. Am. Chem. Soc.* **1980**, *102*, 3816.

(13) (a) Kelly, J. M.; McMurry, T. B. H.; Work, D. N. *J. Chem. Soc., Perkin Trans. 2* **1990**, 981. (b) Kelly, J. F. D.; Doyle, M. E.; Guha, M.; Kavanagh, P. V.; Kelly, J. M.; McMurry, T. B. H. *J. Chem. Soc., Perkin Trans. 2* **1998**, 163.

(14) Mann, J.; Partlett, N. K.; Thomas, A. *J. Chem. Res. (S)* **1987**, 369, and references therein.

(15) Ibuka, T.; Akimoto, N.; Tanaka, M.; Nishii, S.; Yamamoto, Y. *J. Org. Chem*. **1989**, *54*, 4055.

(16) Jiménez, J. M.; Rifé, J.; Ortuño, R. M. *Tetrahedron: Asymmetry* **1996**, *7*, 537.

(17) (a) Costa, J. S.; Dias, A. G.; Anholeto, A. L.; Monteiro, M. D.; Patrocinio, V. L.; Costa, P. R. R. *J. Org. Chem*. **1997**, *62*, 4002. (b) Krief, A.; Provins, L.; Froidbise, A. *Tetrahedron Lett*. **1998**, *39*, 1437, and references therein. (c) Xiang, Y.; Gi, H. J.; Niu, D.; Schinazi, R. F.; Zhao, K. *J. Org. Chem*. **1997**, *62*, 7430. (d) Casas, R.; Parella, T.; Branchadell, V.; Oliva, A.; Ortuño, R. M.; Guingant, A. *Tetrahedron* **1992**, *13*, 2659. (e) Sbai, A.; Branchadell, V.; Ortuño, R. M.; Oliva, A. *J. Org. Chem*. **1997**, *62*, 3049. (f) Guido, G.; Jones, P. G. Pätzel, M. *Tetrahedron: Asymmetry* **1996**, *7*, 2073, and references therein. (g) Busqué, F.; de March, P.; Figueredo, M.; Font, J.; Monsalvatje, M.; Virgili, A.; Álvarez-Larena, A.; Piniella, J. F. *J. Org. Chem*. **1996**, *61*, 8578. (h) Martín-Vilà, M.; Hanafi, N.; Jiménez, J. M.; Álvarez-Larena, A.; Piniella, J. F.; Branchadell, V.; Oliva, A.; Ortuño, R. M. *J. Org. Chem*. **1998**, *63*, 3581. (i) Muray, E.; Álvarez-Larena, Piniella, J. F.; Branchadell, V.; Ortuño, R. M. *J. Org. Chem*. **2000**, *65*, 388.

(18) (a) Jiménez, J. M.; Ortuño, R. M. *Tetrahedron: Asymmetry* **1996**, *7*, 3203. (b) Díaz, M.; Jiménez, J. M.; Ortuño, R. M. *Tetrahedron: Asymmetry* **1997**, *8*, 2465. (c) Rifé, J.; Ortuño, R. M. *Tetrahedron: Asymmetry* **1999**, *10*, 4245. (d) Rifé, J.; Ortuño, R. M. *Org. Lett*. **1999**, *1*, 1221.

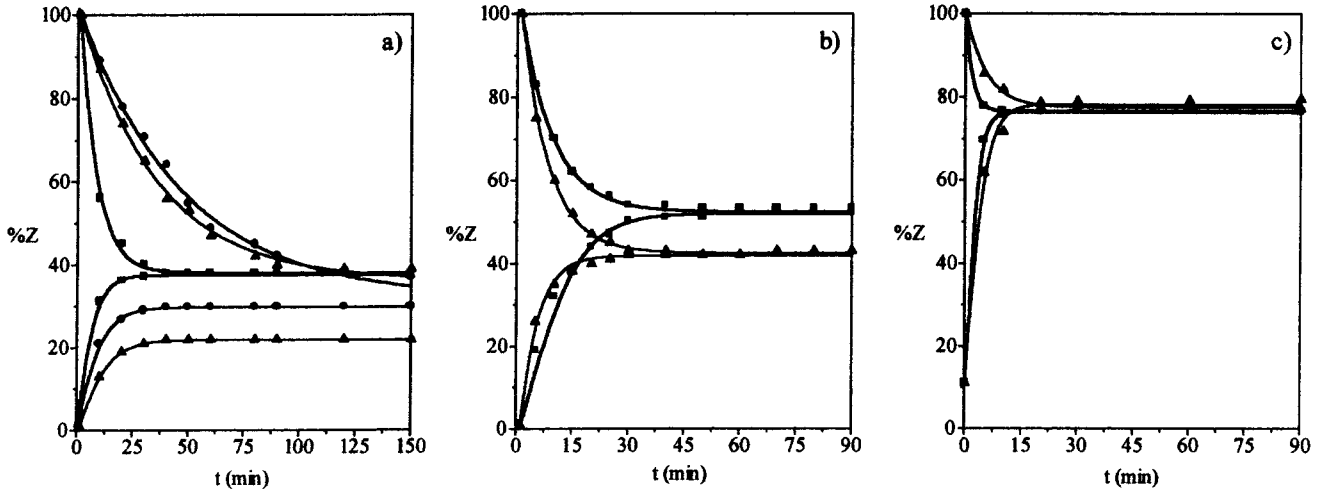

Figure 1. *Z*−*E* Photochemical isomerization of (a) ester **1**, (b) ester **2**, (c) amino ester **3**, in (■) acetone, (●) acetonitrile in the presence of acetophenone (0.1 equiv), (▲) acetonitrile in the presence of benzophenone (0.1 equiv).

Scheme 1

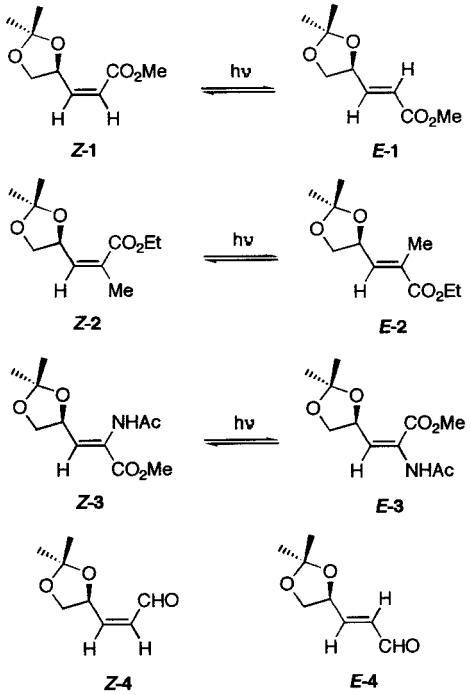

ers. Moreover, the long triplet-lifetimes have been interpreted in terms of T_1-S_0 energy gaps and SOC calculations from the shape of the T_1 potential energy surfaces. Finally, an interpretation of the whole process is provided on the basis of both experimental and theoretical results.

Results and Discussion

1. Stationary Irradiations. *Z* and *E* pentenoates **1**−**3** (Scheme 1) were irradiated in separate experiments as solutions contained in a Pyrex reactor under nitrogen atmosphere, cooled in a dry ice/acetone bath, by using a 125-W medium-pressure mercury lamp. The influence of several solvents and of different photosensitizers was investigated. The presence of a sensitizer was necessary since these compounds do not show absorption bands above 290 nm with λ_{max} between 212 and 236 nm. On the other hand, irradiation of these compounds containing solutions in quartz reactors led to the formation of much unidentified decomposition substances.

Table 1. Photosensitized *Z*−*E* Isomerization of Pentenoates 1−3

entry	pentenoate	sensitizer	solvent	(*Z*/*E*) ratio	time (min)
1	*Z*-**1**	Ph_2CO	MeCN	0.6	120
2	*Z*-**1**	AcPh	MeCN	0.6	120
3	*Z*-**1**	Me_2CO	Me_2CO	0.6[a]	30
4	*E*-**1**	Ph_2CO	MeCN	0.3	120
5	*E*-**1**	AcPh	MeCN	0.4	120
6	*E*-**1**	Me_2CO	Me_2CO	0.6[a]	30
7	*Z*-**2**	Ph_2CO	MeCN	0.7[a]	40
8	*Z*-**2**	Me_2CO	Me_2CO	1.1[a]	60
9	*E*-**2**	Ph_2CO	MeCN	0.7[a]	40
10	*E*-**2**	Me_2CO	Me_2CO	1.1[a]	60
11	*Z*-**3**	Ph_2CO	MeCN	3.5[a]	25
12	*Z*-**3**	Me_2CO	Me_2CO	3.2[a]	10
13	*E*-**3**	Ph_2CO	MeCN	3.5[a]	25
14	*E*-**3**	Me_2CO	Me_2CO	3.2[a]	10

[a] Photostationary state ratio.

Some extent of *Z*−*E* isomerization was found when acetonitrile or ethyl acetate 0.08 M solutions of pure *Z*- or *E*-**1** were irradiated in the presence of 0.1 equiv of acetophenone or benzophenone, the processes being very slow (Figure 1a. Table 1, entries 1, 2, 4, 5). The behavior of these pentenoates changed dramatically when irradiated in acetone, the photostationary state being reached in 30 min with an associated ratio $(Z/E)_{PSS} = 0.6$ (Figure 1a, Table 1, entries 3, 6). Obviously, in this case acetone plays both the roles of the solvent and the photosensitizer.

In other sets of experiments, *Z* and *E* pentenoates **2** were irradiated as acetonitrile or dichloromethane 0.02 M solutions in the presence of benzophenone (0.1 equiv). The photostationary state ratio $(Z/E)_{PSS} = 0.7$ was reached in about 40 min. The isomerization rate was slightly slower in acetone solutions and $(Z/E)_{PSS} = 1.1$ (Figure 2b, Table 1, entries 7−10). Finally, aminopentenoates **3** isomerized faster than **1** and **2** in either acetone or acetonitrile solutions, the last one in the presence of benzophenone, reaching the photostationary ratios $(Z/E)_{PSS}$ of 3.5 and 3.2, respectively (Tables 1, entries 11−14).

From these results, we assumed that the photoinduced *Z*−*E* isomerization of these pentenoates, under the above conditions, requires a photosensitizer to promote the substrate to an excited state, presumably the T_1 state. The intermediacy of such transients was confirmed by

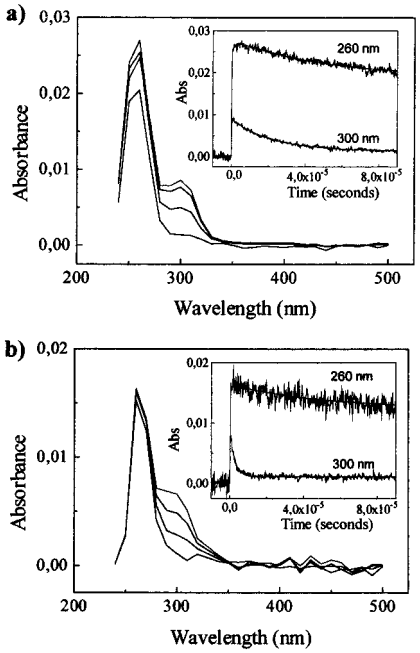

Figure 2. (a) Transient absorption spectrum (λ_{ex} = 266 nm) of a nitrogen-purged acetonitrile solution of ***Z*-1**. From top to bottom: 1×10^{-6}, 4×10^{-6}, 16×10^{-6}, 90×10^{-6} s after the laser flash. Inset: decay traces at 260 and 300 nm. (b) Transient absorption spectrum (λ_{ex} = 266 nm) of a nitrogen-purged acetonitrile solution of ***E*-1**. From top to bottom: 1×10^{-6}, 2×10^{-6}, 4×10^{-6}, 90×10^{-6} s after the laser flash. Inset: decay traces at 260 and 300 nm.

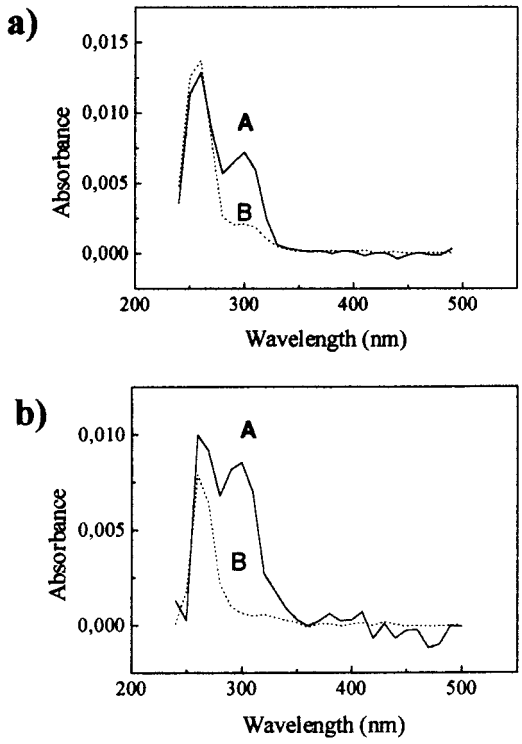

Figure 3. Fitted spectra for transients **A**, **B** obtained by Global Analysis of the complete kinetic data of the decays for the transient absorption of (a) *Z*-**1** and (b) *E*-**1**.

laser flash-photolysis experiments allowing the quenching rate constants for the employed photosensitizers to be determined, whereas theoretical calculations offered an interpretation of the whole process.

It is noticeable that in all these experiments only *Z*/*E* isomers were found and [2 + 2] cycloadducts or other photoproducts were never detected.

2. LFP Studies. Several experiments were performed on pentenoates **1**−**3** as acetonitrile solutions contained in quartz cells which were irradiated at 266 nm. The transient absorption spectra of *Z*- and *E*-**1** and the results from global analysis are presented in Figures 2 and 3, respectively. Figure 2b shows the transient absorption spectrum of pure *E*-**1** as well as the decay traces at 300 and 260 nm. These traces show very different kinetics (a fast decay at 300 nm and a slow one at 260 nm), and two species seem to be involved. According to GLint global analysis of the complete kinetic decays set,[19a] two transients, **A** and **B**, are involved, transient **B** being formed from **A**. Transient **A** presents maxima at 300 and 260 nm whereas **B** maximizes at 260 nm (Figure 3b).[19b] Their estimated lifetimes are 2.5 μs and 1.3 ms, respectively, and they are not dependent on the pentenoate concentration (the self-quenching process is negligible). GLint analysis also showed that decays of both species are first-order**.** With the purpose of clarifying whether any of them is a triplet, we performed some experiments with triplet−triplet sensitizers (benzophenone and acetophenone) and a triplet quencher (naphthalene).

(19) (a) Carey, M. *EPA Newsletter* **1994**, *52*, 21. (b) GLint analysis allows the interpretation of experimental decays at 260 nm (insets in Figures 2 and 4) as the result of two combined kinetics: a growing kinetics for B and a decreasing kinetics for A.

Table 2. Quenching Rate Constants of Benzophenone and Acetophenone Triplets by *Z/E* Enoates 1−3

	k_q ($\times 10^8$ l mol^{-1} s^{-1})	
enoate	benzophenone	acetophenone
E-**1**	0.4	7.8
Z-**1**	0.7	17.7
Z-**2**	3.5	21.9
E-**2**	4.6	32.1
Z-**3**	9.5	38.9

Compound *E*-**1** quenched the transient triplets of both benzophenone and acetophenone when used as sensitizers. Stern−Volmer plots of the observed rate constants for the benzophenone or acetophenone-triplet decay vs pentenoate concentration were linear in all cases. Table 2 shows the determined quenching constants. Although they resulted to be very small, k_q for acetophenone was larger than k_q for benzophenone, in good accordance with the results from stationary irradiations.

Quenching by naphthalene was also investigated. Owing to the strong absorption of naphthalene at the wavelength of the pulsed laser (266 nm), a low concentration of this quencher was used to ensure that more than 80% of the exciting light at 266 nm was absorbed by the pentenoate. The following observed effects are noticeable: (i) Transient **A** decays faster when the quencher is added. (ii) The absorbance of transient **B** decreases markedly thus suggesting that **B** results from **A**, in good accordance with the global analysis. In addition, the transient absorption of the naphthalene triplet was strongly enhanced when a small amount of *E*-**1** was added. Therefore, we assigned these effects to an efficient deactivation of **A** by naphthalene as a triplet quencher.

As **A** deactivates triplet sensitizers and, in turn, undergoes deactivation by a triplet quencher, we can

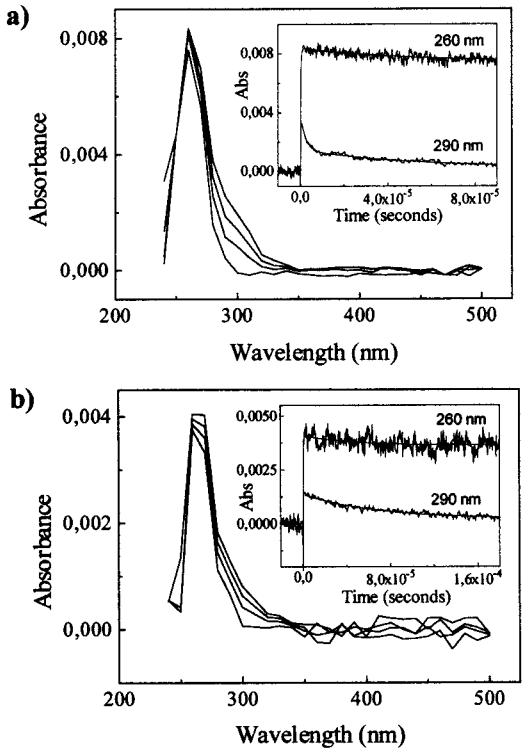

Figure 4. (a) Transient absorption spectrum ($\lambda_{ex} = 266$ nm) of a nitrogen-purged acetonitrile solution of *Z*-**2**. From top to bottom: 2×10^{-6}, 4×10^{-6}, 16×10^{-6}, 90×10^{-6} s after the laser flash. Inset: decay traces at 260 and 300 nm. (b) Transient absorption spectrum ($\lambda_{ex} = 266$ nm) of a nitrogen-purged acetonitrile solution of *E*-**2**. From top to bottom: 4×10^{-6}, 6×10^{-6}, 32×10^{-6}, 64×10^{-6} s after the laser flash. Inset: decay traces at 260 and 290 nm.

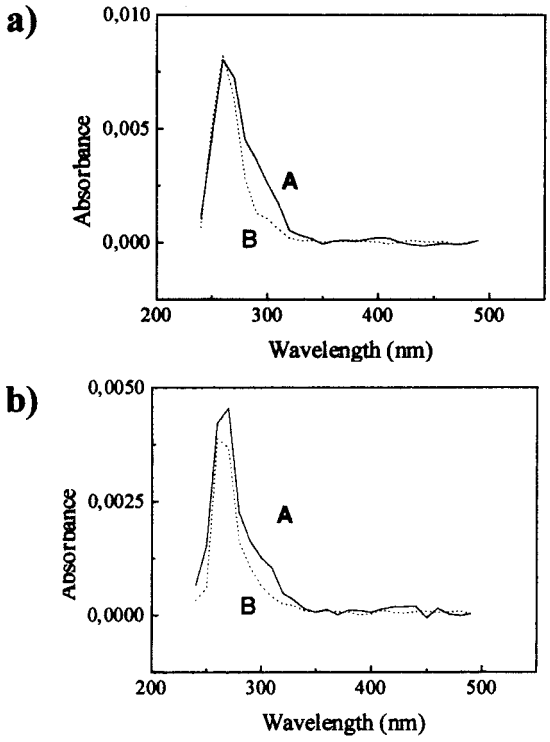

Figure 5. Fitted spectra for transients **A**, **B** obtained by Global Analysis of the complete kinetic data for the decays of the transient absorption of (a) *Z*-**2** and (b) *E*-**2**.

conclude that species **A** is a triplet. Species **B** could be the precursor of the unidentified substances obtained under stationary irradiations of pentenoate solutions contained in quartz reactors. In the literature, similar species have been detected in the 260−280 nm region, upon pulse excitation of cyclic enones, their nature having not been unambiguously assigned.[9]

The transient behavior of *Z*-**1** is similar to that of *E*-**1**. Figure 2a shows the transient absorption spectrum of the *Z* isomer as well as the decay traces at 300 and 260 nm. Again, GLint analysis (Figure 3a) showed the presence of two species, **A** and **B**, with lifetimes of 16.3 μs and 0.47 ms, respectively. The rate constants for *Z*-**1** promoted deactivation of excited benzophenone and acetophenone are shown in Table 2.

Pentenoate **2**, as both *Z* and *E* isomers, showed a transient behavior similar to pentenoates **1** (Figure 4). GLint analysis (Figure 5) allowed us to deduce the spectra for transients **A** and **B**. The lifetimes determined for the corresponding triplets were 2.8 μs for *Z*-**2** and 11.8 μs for *E*-**2**.

In addition, pentenoates *Z*- and *E*-**2** resulted to be more efficient than any isomer of pentenoates **1**, but less effective than *Z*-**3**, in the deactivation of triplet benzophenone or triplet acetophenone as deduced from inspection of Table 2.

From all these results, we can state that the *Z*−*E* photoisomerization of pentenoates **1**−**3** takes place via triplet species. Their lifetimes are in the range of 2−16 μs, considerably longer than values reported for simple enones (ca. 8−400 ns).[9] Since the different behavior of olefins conjugated to a carbonyl or to an alkoxycarbonyl group could be related to the flexibility of the molecules in the triplet state, we decided to perform theoretical calculations as described below.

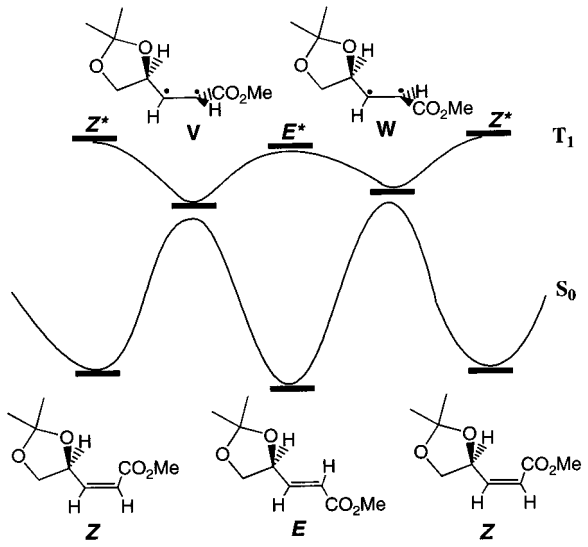

Figure 6. Schematic energy profiles corresponding to rotation around the C2−C3 bond of **1** for the S_0 and T_1 states.

3. Theoretical Calculations. We have studied the rotation around the C=C bond for the S_0 and T_1 states of **1**. The corresponding schematic energy profiles are presented in Figure 6. For the S_0 potential energy surface we have optimized the geometries of the *Z* and *E* isomers. Due to the presence of a stereogenic center in **1**, two diastereomeric chiral structures, **V** and **W**, which correspond to torsion angles of about 90 and −90 degrees,

Table 3. Selected Geometry Parameters[a] for Stationary Points of the S_0 and T_1 Potential Energy Surfaces of 1

state	structure[b]	C1−O1	C2−C1	C3−C2	C4−C3−C2−C1	C5−C4−C3−C2
S_0	*Z*	1.233	1.484	1.354	0.5	88.1
	E	1.229	1.488	1.349	179.3	−108.7
T_1	*Z**	1.260	1.430	1.496	−6.0	92.8
	V	1.238	1.465	1.460	−76.3	96.7
	*E**	1.255	1.430	1.502	179.7	−69.3
	W	1.239	1.464	1.462	81.3	−91.2

[a] See Figure 7 for atom numbering. Bond lengths in Å and dihedral angles in degrees. [b] See Figure 6.

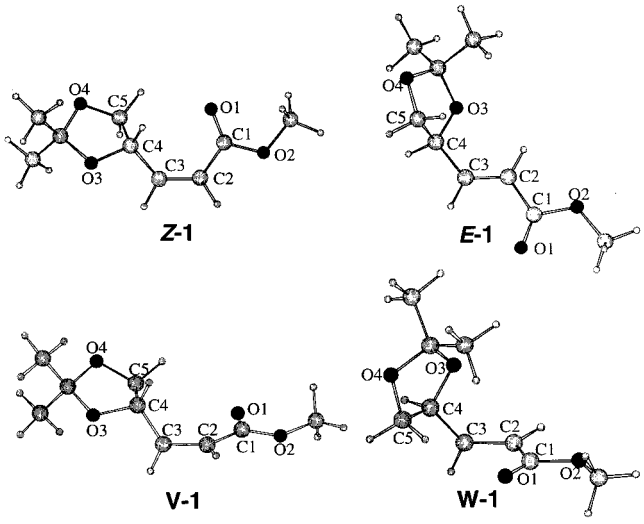

Figure 7. Optimized geometries of the energy minima corresponding to the S_0 (*Z*-**1** and *E*-**1**) and T_1 (**V-1** and **W-1**) potential energy surfaces of **1**.

Table 4. Computed Energies[a] for Several Structures[b] of the S_0 and T_1 States of the Studied Enoates

enoate	state	*Z*(*Z**)	V	*E*(*E**)	W
1	S_0	0.7		0.0	
	T_1	69.8	60.0	69.7	60.3
2	S_0	0.0		0.4	
	T_1	65.5	56.5	66.4	56.5
3	S_0	0.0		0.6	
	T_1	57.9	48.8	56.7	47.2

[a] Relative to the ground state of the most stable isomer. In kcal mol^{-1}. [b] See Figure 6.

have been located in the T_1 surface as two energy minima. Any of these two structures is accessible from either *Z* or *E* ground-state isomers. We have also located the *Z** and *E** structures, corresponding to transition states connecting **V** and **W**. The geometries of *Z*-**1**, *E*-**1**, **V-1**, and **W-1** are represented in Figure 7 and values of selected geometry parameters corresponding to these structures are shown in Table 3.

Table 3 shows that in the triplet structures the C_2-C_3 bond has lost its double bond character. In **V-1** and **W-1**, the C_1-O_1 bond length has only slightly increased with respect to the ground state values. This result shows that the unpaired electrons are mainly located at the C_2 and C_3 atoms, with very little delocalization to the carbonyl group. On the other hand, the values of C_1-O_1 and C_1-C_2 bond lengths in the transition states *Z**-**1** and *E**-**1** reveal a slightly larger electron delocalization.

Stationary points in the S_0 and T_1 potential energy surfaces have also been located for compounds **2** and **3**. Table 4 presents the energies computed for the studied structures of the S_0 and T_1 potential energy surfaces of esters **1**−**3**.[20]

Table 5. Computed Energies[a] for Several Structures[b] of the S_0 and T_1 States of 4

state	*Z*(*Z**)	V	*E*(*E**)	W
S_0	0.5		0.0	
T_1	53.5	56.8	59.2	56.9

[a] Relative to the ground state of the most stable isomer. In kcal mol^{-1}. [b] The structure notation is the same as in Figure 6.

The obtained results are very similar for the three molecules. The main difference is found for the ground state, since *E*-**1** is more stable than *Z*-**1**, whereas the *Z* isomer is the more stable one, both for **2** and **3**. The adiabatic singlet to triplet excitation energy goes down as we move from **1** to **2** and to **3**. This result is in excellent agreement with the relative values of acetophenone and benzophenone quenching rate constants shown in Table 2.

The computed energies can also be related to the observed $(Z/E)_{PSS}$ ratios shown in Table 1. As it is well-known, the $(Z/E)_{PSS}$ ratio depends on the rate constants for quenching of the sensitizer by the *Z* and *E* isomers and on the rate constants for decay of triplet enoate to *Z* and *E* ground states. For high energy sensitizers, one can assume that energy transfer occurs at close to the diffusion-controlled rate, so that the composition of the isomer mixture depends only on the rate of decay of triplet enoate. Actually, Table 1 shows that, for all enoates, the results obtained with acetone as sensitizer are in accordance with the ground state *Z*/*E* relative energies presented in Table 4. For enoate **2**, benzophenone reverses the $(Z/E)_{PSS}$ ratio with respect to acetone. Finally, for **3**, which has the lowest triplet energy, both acetone and benzophenone lead to the same $(Z/E)_{PSS}$ ratio.

As mentioned above, the enoates considered in this work have triplet lifetimes several orders of magnitude larger than what has been previously observed for other α,β-unsaturated carbonyl compounds. To get a better understanding, we have extended our theoretical study to methyl pentenoate and to aldehyde **4** (Scheme 1). The results obtained for methyl pentenoate are very similar to those presented for ester **1**, whereas the results corresponding to **4**, summarized in Table 6, are rather different, since the *Z**-**4** and *E**-**4** structures are energy minima. We have not located the transition states linking the minima of the T_1 potential energy surface of **4**, but they are expected to involve smaller energy barriers than those computed for ester **1**. The most significant geometry parameters corresponding to the structures optimized for **4** are shown in Table 6. The values of the C_1-O_1 and C_1-C_2 bond lengths in the *Z**-**4** and *E**-**4** structures indicate

(20) For **1**, we have calculated zero point energies, thermal corrections to the energy, and entropies for all stationary points. For the ground state, the entalpy difference (0 K and 1 atm) and the Gibbs energy difference (298 K and 1 atm) between *E*-**1** and *Z*-**1** are, respectively, 0.8 and 0.7 kcal mol^{-1}. These values are very similar to the potential energy difference shown in Table 4.

Table 6. Selected Geometry Parameters[a] for Stationary Points of the S_0 and T_1 Potential Energy Surfaces of 4

state	structure[b]	C1−O1	C2−C1	C3−C2	C4−C3−C2−C1	C5−C4−C3−C2
S_0	*Z*	1.236	1.479	1.360	1.2	88.1
	E	1.232	1.486	1.353	179.4	−109.2
T_1	*Z**	1.316	1.414	1.399	3.0	112.7
	V	1.251	1.449	1.461	−71.8	96.4
	*E**	1.300	1.425	1.412	−179.4	118.5
	W	1.251	1.449	1.464	79.2	−89.1

[a] See Figure 8 for atom numbering. Bond lengths in angstroms and dihedral angles in degrees. [b] The structure notation is the same as in Figure 6.

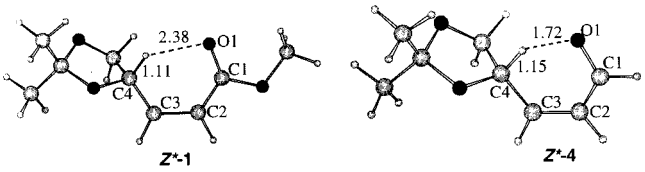

Figure 8. Optimized geometries of the ***Z**** structures corresponding to the T_1 potential energy surfaces of **1** (transition state) and **4** (energy minimum). Selected interatomic distances in Å.

a significant electron delocalization. The atomic spin populations obtained from Mulliken population analysis show that the unpaired electrons are mainly located in O_1 and C_3, while in **V-4**, **W-4**, and all the triplet structures of ester **1** the maximum spin populations are obtained for C_2 and C_3. These results suggest that *Z**-**4** and *E**-**4** correspond to n−π* instead of $\pi-\pi$* excited states.

Moreover, Table 6 shows that there is a relatively important energy difference between the *Z**-**4** and *E**-**4** structures, in such a way that *Z**-**4** becomes the absolute minimum of the T_1 energy surface. Figure 8 presents the optimized geometries of the *Z**-**1** and *Z**-**4** structures. As we can observe, in **4** there is a strong interaction involving the hydrogen at C_4 and the carbonyl oxygen atom.[21] Such an interaction does not exist in **1**. This kind of structure has also been obtained for methoxycrotonaldehyde, but not for crotonaldehyde. Thus, both the presence of the aldehyde group and of an oxygen atom bonded to C_4 seem to contribute to this additional stabilization.

Let us now discuss the T_1 to S_0 decay. This process takes place through spin−orbit coupling. According to Salem and Rowland,[22] there are two fundamental prerequisites for effective intersystem crossing between a triplet and a singlet state. First, there must be a nonzero mixing of the electronic wave functions through the spin−orbit interaction operator. Moreover, the separation between the singlet and triplet levels must not be too large. Salem and Rowland[22] have also analyzed the dependence of SOC on the molecular structure using a two electrons in two orbitals model. More recently, Michl has analyzed the validity of this model.[23]

We have computed the SOC and the T_1-S_0 energy gap for the stationary points (*Z**, **V**, *E**, and **W**) as well as for intermediate points corresponding to C_2-C_3 torsion angles of ±45 and ±135° of the T_1 potential energy surface of ester **1**. The results obtained are represented in Figure 9. For each point of the T1 potential energy surface, the energy of the singlet state has been estimated from spin-unrestricted BLYP calculations by breaking the spatial symmetry between α and β electron densities. The result of this calculation corresponds to a mixture of singlet and triplet states from which the singlet energy can be obtained through spin-projection.[24]

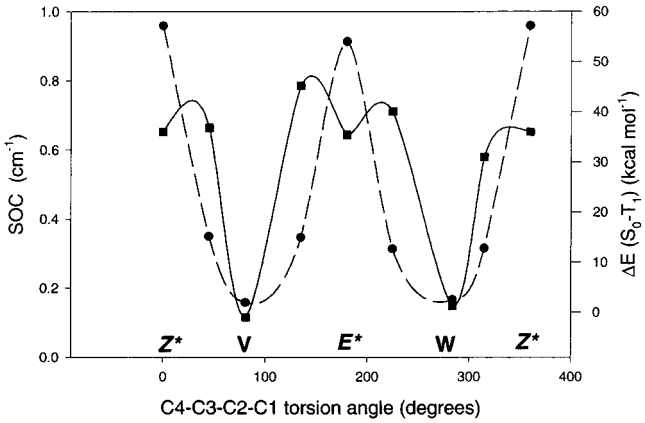

Figure 9. Variation of the computed S_0-T_1 energy gap (dashed line) and spin−orbit coupling (solid line) of **1** with the torsion around the C2−C3 bond.

Figure 9 shows that SOC is negligible in the energy minima, **V-1** and **W-1**, where the T_1-S_0 gap is the smallest one. This result is in accordance with results reported by Caldwell et al. for ethylene.[8] SOC reaches its maximum for structures halfway between these minima and the transition states *Z** and *E**, as it is also observed for ethylene.[8]

The isc probability should be very small for both the minima **V-1** and **W-1**, due to negligible SOC, and also for the transition states *Z**-**1** and *E**-**1**, due to a too large T_1-S_0 energy gap. Therefore, this process is expected to take place for intermediate C_2-C_3 torsion angles. The shape of the T_1 potential energy surface (see Figure 6 and Table 4) shows that the system has to overcome an energy barrier to achieve these structures. Therefore, triplet lifetimes for compounds **1**−**3** are expected to be relatively long. On the other hand, the T_1 potential energy surface for aldehyde **4** is very flat (see Table 5) and the energy necessary to achieve structures with a large isc probability is expected to be much lower. This feature would lead to a shorter triplet lifetime for this compound. Moreover, as we have already mentioned, the planar structures *Z**-**4** and *E**-**4** correspond to n-π* triplets. These structures could undergo isc to the n-π* S_1 state, so that the decay of triplet **4** would be faster than for enoates **1**−**3**.

A similar result has been obtained for methyl vinyl ketone, where the experimentally determined triplet

(21) This is the same interaction involved in a Norrish Type II process.

(22) Salem, L.; Rowland, C. *Angew. Chem., Int. Ed. Engl.* **1972**, *11*, 92.

(23) Michl, J. *J. Am. Chem. Soc.* **1996**, *118*, 3568.

(24) (a) Goldstein, E.; Beno, B.; Houk, K. N. *J. Am. Chem. Soc.* **1996**, *118*, 6036. (b) Yamaguchi, K.; Jensen, F.; Dorigo, A.; Houk, K. N. *Chem. Phys. Lett.* **1988**, *149*, 537.

lifetime is 8 ns.[12] The T_1 potential energy surface is also very flat and presents two energy minima corresponding to the orthogonal and to the planar structures. The orthogonal structure is the absolute minimum, and the planar one is only 2.8 kcal mol^{-1} higher in energy. We can conclude, therefore, that the considerably longer triplet lifetimes determined for esters **1** and **2** is mainly due to the relatively high energy-barriers between the orthogonal triplets (energy minima) and the planar transition state structures *Z** and *E**, in every case.

Concluding Remarks

Several conclusions emerge from this study. We have shown, by means of stationary irradiations and LFP experiments, that *Z*−*E* photoisomerization of the chiral pentenoates **1**−**3** takes place through excited triplet states of unexpectedly long lifetimes. Quenching rate constants of benzophenone and acetophenone triplets by these compounds suggest that their triplet energies decrease when moving from **1** to **3**, in good accordance with the computational results.

The potential energy surfaces of **1**−**3** present two energy minima, corresponding to orthogonal diastereomeric chiral triplets while the planar triplets are transition states. The torsional barriers are in the range of 8−10 kcal mol^{-1}. The calculation of the T_1−S_0 energy gap and SOC at different points of the T_1 potential energy surface of **1** shows that decay to the ground state does not occur from the orthogonal triplets, but from structures with C−C torsional angles of about ±45° with respect to the orthogonal minima. Then, an energy barrier of 4−5 kcal mol^{-1} must be overcome to reach these structures. This barrier is much higher than that estimated for aldehyde **4** and for methyl vinyl ketone in which the planar triplets are also energy minima and close in energy to the orthogonal ones due to electron delocalization on the carbonyl group. Consequently, the energy barrier necessary to reach structures with a high isc probability is expected to be lower for aldehydes and ketones than for enoates. The longer triplet lifetimes determined by LFP for α,β-unsaturated esters can be, therefore, understood on the basis of these results.

Experimental Section

Enoates **1**−**3** were synthesized according to the procedures described in the literature[14−16] and purified by flash-chromatography (silica gel) followed by preparative HPLC (Prep Pak Cartridge 25 × 100 mm, Bondapak C_{18}, 15−20 μm). Commercial solvents of spectroscopic grade were used. Sample solutions were purged with argon for 10−15 min prior to the experiments.

Monitoring of stationary irradiations and isomeric ratio determinations were carried out by GC for **1** and **2** and by HPLC for **3**.

The nanosecond LFP experiments were performed by using an LKS50 instrument from Applied Photophysics. Pulses of ca. 9 ns and energies of 15−20 mJ were provided by a Q-switched Nd:YAG laser (Spectron Laser Systems, UK). All experiments were carried out on nitrogen-saturated acetonitrile solutions contained in quartz cells. The transient difference absorption spectra were obtained by recording the transient decays at different analyzing wavelengths. Typically, the data from 4 to 10 laser pulses (depending on the signal-to-noise ratio), at 266 nm, were averaged prior to computer processing. In addition, global analysis of the complete kinetic data set of the decays was carried out by using GLint, which is a form of global analysis developed by Applied Photophysics Ltd. that uses the Marquardt−Levenberg algorithm and fourth-order Runge−Kutta numerical integration.[19]

Sensitizing experiments were performed with sensitizers in acetonitrile solutions. Aliquots of each dissolved pentenoate were added by using a microliter syringe. The naphthalene quenching of pentenoate **1** was performed on a 5:1 olefin−naphthalene molar-ratio solution.

Computational Details. Molecular geometries have been optimized for the ground state and for the first triplet state of the studied olefins by means of density functional calculations (DFT) using Becke's[25] functional for exchange and the functional of Lee, Yang, and Parr[26] for correlation (BLYP) with the standard 6-31G(d) basis set.[27] For triplets, we have adopted a spin-unrestricted formalism. All these calculations have been done using the Gaussian-98 program.[28] We have selected the BLYP functional since it yields vertical and adiabatic singlet to triplet excitation energies for ethylene in excellent agreement with those obtained at a higher level of calculation.[29] Moreover, it has been recently shown by Brink et al.[30] that the BLYP method leads to excellent results for the T_1 potential energy surface of butadiene and hexatriene.

Spin−orbit coupling between T_1 and S_0 states has been calculated at several points of the T_1 potential energy surface using the full Breit−Pauli spin−orbit operator[31] with the procedure implemented in the GAMESS program.[32] In these calculations, the T_1 wave function has been calculated at the restricted open shell Hartree−Fock level of theory (ROHF), while for the S_0 wave function, a configuration interaction (CI) with complete active space of two electrons in two orbitals has been done. The orbitals in the CI calculations are those corresponding to the ROHF calculations of T_1. The computation of quantitatively accurate spin−orbit coupling requires the use of higher levels of calculation which are not possible with our computational resources. We expect, however, the results to be qualitatively correct.

Acknowledgment. Authors are grateful to Prof. Rafael Suau, Universidad de Málaga, for reading the manuscript. Financial support from DGESIC (PB97-0214) and computer time from the Centre de Supercomputació de Catalunya are gratefully acknowledged. E.G.-E. and J.R. thanks the CIRIT, and R.G.-M., M.M.-V., and E.M. thank the MEC for respective predoctoral fellowships.

Supporting Information Available: Total energies and geometries of the optimized structures for enoates **1**−**3**, and aldehyde **4**. This material is available free of charge via the Internet at http://pubs.acs.org.

JO000549G

(25) Becke, A. D. *J. Chem. Phys.* **1993**, *98*, 1372.
(26) Lee, C.; Yang, W.; Parr, R. G. *Phys. Rev. A* **1988**, *37*, 785.
(27) Hehre, W. J.; Radom, L.; Schleyer, P. v. R.; Pople, J. A. *Ab Initio Molecular Orbital Theory*; Wiley: New York, 1986.
(28) Frisch, M. J.; Trucks, G. W.; Schlegel, H. B.; Scuseria, G. E.; Robb, M. A.; Cheeseman, J. R.; Zakrzewski, V. G.; Montgomery, J. A., Jr.; Stratmann, R. E.; Burant, J. C.; Dapprich, S.; Millam, J. M.; Daniels, A. D.; Kudin, K. N.; Strain, M. C.; Farkas, O.; Tomasi, J.; Barone, V.; Cossi, M.; Cammi, R.; Mennucci, B.; Pomelli, C.; Adamo, C.; Clifford, S.; Ochterski, J.; Petersson, G. A.; Ayala, P. Y.; Cui, Q.; Morokuma, K.; Malick, D. K.; Rabuck, A. D.; Raghavachari, K.; Foresman, J. B.; Cioslowski, J.; Ortiz, J. V.; Stefanov, B. B.; Liu, G.; Liashenko, A.; Piskorz, P.; Komaromi, I.; Gomperts, R.; Martin, R. L.; Fox, D. J.; Keith, T.; Al-Laham, M. A.; Peng, C. Y.; Nanayakkara, A.; Gonzalez, C.; Challacombe, M.; Gill, P. M. W.; Johnson, B.; Chen, W.; Wong, M. W.; Andres, J. L.; Gonzalez, C.; Head-Gordon, M.; Replogle, E. S.; Pople, J. A.8 *Gaussian 98*, Revision A.5; Gaussian, Inc.: Pittsburgh, PA, 1998.
(29) Using geometries optimized at the QCISD/6-31G(d) level of calculation, vertical (adiabatic) excitation energies are 105.8 (65.7) kcal mol^{-1} at the BLYP/6-31-G(d) level, 104.7 (66.3) kcal mol^{-1} at the BLYP/cc-pVTZ level, and 104.0 (67.8) kcal mol^{-1} at the CCSD(T)/cc-pVTZ level.
(30) Brink, M.; Johnson, H.; Ottosson, C.-H. *J. Phys. Chem. A* **1998**, *102*, 6513.
(31) (a) Furlani, T. R.; King, H. F. *J. Chem. Phys.* **1985**, *82*, 5577. (b) King, H. F.; Furlani, T. R. *J. Comput. Chem.* **1988**, *9*, 771.
(32) Lee, C.; Yang, W.; Parr, R. G. *Phys. Rev. A* **1988**, *37*, 785.